NJC

PAPER

View Article Online
View Journal

Cite this: DOI: 10.1039/c7nj03471g

Metal- and catalyst-free, one-pot, three-component synthesis of propargylamines in magnetized water: experimental aspects and molecular dynamics simulation

Mohammad Bakherad, *[a] Fatemeh Moosavi, *[b] Rahele Doosti, [a] Ali Keivanloo [a] and Mostafa Gholizadeh [b]

Received 12th September 2017,
Accepted 8th February 2018

DOI: 10.1039/c7nj03471g

rsc.li/njc

Magnetized water (MW), as a green-promoting medium, is applied for the one-pot, metal- and catalyst-free, practical, efficient, and environmentally benign three-component reactions of aldehydes, amines, and alkynes. The salient features of this novel methodology are its simplicity, low cost, short reaction time, high reaction yield, easy work-up, and absence of hazardous organic solvents. Moreover, the molecular dynamics (MD) simulation as well as the experimental results confirm that MW leads to strong interactions between the reagents to produce the products. From another point of view, hydrogen bond interactions play a crucial role in conducting the reactions towards appropriate products.

Introduction

Among all the existing multi-component reactions, a three-component coupling of an aldehyde, an amine, and an alkyne (A^3-coupling) is an appealing approach to the preparation of propargylamines, which have found wide applications as precursors for non-identical nitrogen-containing compounds like pyrroles,[1] pyrrolidines,[2] indolizine,[3] and oxazoles.[4] There are several classical methods available for the preparation of propargylamines.[5] These methods, however, have a number of shortcomings like the need for controlled reaction conditions and a stoichiometric amount of metal reagents, and moisture sensitivity. To overcome these problems, the transition metal-catalyzed three-component coupling of an aldehyde, an amine, and an alkyne has been proposed and broadly used under mild conditions (Scheme 1). Thus there has been much effort to develop effective transition metal catalysts for the activation of the C–H bond in terminal alkynes. Several transition metals such as ruthenium, copper,[6] silver,[7] indium,[8] iridium,[9] and gold[10] have been used in such three-component reactions. In this regard, we have recently reported the synthesis of propargylamines catalyzed by an eggshell-supported-Cu(II) salophen complex under solvent-free conditions.[11] However, several catalytic methods have been reported for the preparation of propargylamines, most of which require an inert gas, an organic solvent, a high temperature, and an expensive metal such as Au, Ag, Ir, or Ru, as the catalyst. Moreover, the use of metal catalysts often affords a Glaser homo-coupling compound as a by-product, which gives rise to a decrease in the reaction yield. Also transition metal catalysts give rise to the release of metal waste in the process. Thus the establishment of a metal-free system is required.

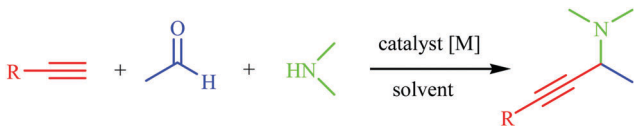

Scheme 1 Synthesis of propargylamines catalyzed by transition metals.

Lee *et al.*[12] have developed metal-free conditions for the synthesis of propargylamines from the one-pot, three-component reaction of aldehydes, amines, and alkynyl carboxylic acids in CH_3CN, as the solvent. Patil and co-workers[13] have reported a metal-free base-catalyzed A^3-coupling in the presence of catalytic tetraalkylammonium hydroxide in DMSO, as the solvent, which is not a good one for the purification step. Moreover, Sreedhar *et al.*[14] have developed a metal-free protocol for the synthesis of propargylamines *via* the three-component coupling of various dihalomethanes, secondary amines, and alkynes in dichloromethane at 70 °C for 12 h. However, many of these synthetic methods face a number of disadvantages like using toxic solvents and basic conditions, and having tedious steps, low reaction yields, and long reaction times, which limit their use in practical applications. In order to overcome these problems, the development of a catalyst-free, milder, cheaper, and highly-efficient

[a] Faculty of Chemistry, Shahrood University of Technology, Shahrood 3619995161, Iran. E-mail: m.bakherad@yahoo.com
[b] Department of Chemistry, Faculty of Science, Ferdowsi University of Mashhad, Mashhad 91779, Iran. E-mail: moosavibaigi@um.ac.ir

method as well as an environmentally benign one is desirable for the synthesis of propargylamines.

Recently, the center of attention in ''green chemistry'' using environmentally friendly reagents and conditions has been a very interesting development in the preparation of broadly used organic compounds. Using water as a favorable solvent for organic reactions has gained an appreciable interest in organic synthesis due to its green credentials.[15] On the other hand, water is an odd compound showing an exclusive selectivity and reactivity, considering the amount of oxygen dissolved in its solutions and the intermolecular hydrogen bonding formed between the molecules.[16] These features allow water to act as a catalyst, a solvent or a reactant, which is different from those seen in conventional organic solvents. Most chemical reactions, however, could not be carried out in water, as a solvent, because they require the presence of catalysts or reagents.

Water can be magnetized in the presence of an external magnetic field, and due to the magnetization, many properties of water such as density, penetration, specific heat, refractive index, electric dipole moment, vaporization enthalpy, surface tension, and viscosity change compared with non-magnetic water.[17] On the basis of literature surveys carried out on MW during the past few years, most researchers have been interested in studying the effect of an applied magnetic field on the properties of water, especially the hydrogen bond distribution.[18] In addition, a number of researchers have investigated the effect of MW on the morphology of precipitated calcium carbonate,[19] TiO_2-based varistors,[20] and preparation of manganese oxide nanocrystals.[21] Very recently, we have reported the synthesis of pyrano[2,3-*c*]-pyrazoles,[22a] pyrazolo pyranopyrimidines,[22b] and diuracilopyrans[22c] using MW, as a solvent.

To shed light on the extent of enhanced hydrogen bonding and local environmental structures, MD simulation has been applied as a powerful tool. MD is able to decrypt the local structures around individual atoms and molecules to comprehend the process at the molecular level. However, as far as the authors are aware, up to the present time, no information has been offered by MD simulation for a specific effect of magnetized water on the synthesis of propargylamines, although an MD research study has shown that magnetized water plays a crucial role in the reaction between aldehydes and barbituric acid at low temperatures.[22c]

In view of these considerations, knowledge of the process from a molecular viewpoint may be used to determine the effect of magnetized water on the conduction of an understudied reaction. All the simulations were analyzed using the radial distribution functions, *z* density profile, and molecular mobility.

Here, we wish to report the metal- and catalyst-free synthesis of propargylamines **4** *via* one-pot three-component reactions of various alkynes **1**, aldehydes **2**, and amines **3** in MW (Scheme 2). Moreover, the effect of MW in the synthesis of propargylamines was investigated by theoretical studies.

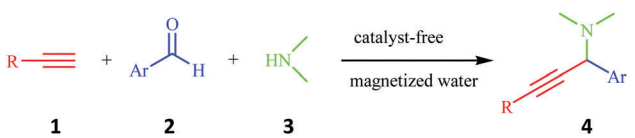

Scheme 2 Catalyst-free synthesis of propargylamines in MW.

Results

Magnetized water was prepared using a static magnetic system of 0.6 T field strength with a flow rate of 500 mL s^{-1} at different magnetic field time exposures (Fig. 1).[22] Doubly distilled water, deionized by a Millipore Q-Plus 185 system, was used throughout the experiments.

A test-reaction was performed using benzaldehyde (1 mmol), piperidine (1.2 mmol), and phenyl acetylene (1.5 mmol) in water at room temperature in the absence of an applied magnetic field in order to establish the effectiveness of MW. No conversion to the product was obtained even after 5 h (Table 1, entry 10). To optimize the reaction conditions, the above model reaction was carried out under different reaction conditions. As indicated in this table, the magnetization time plays a critical role in obtaining a high yield of product **4a**. The best reaction yield of **4a** was found in water magnetized for ten minutes and with a reaction time of 120 minutes at 60 °C (Table 1, entry 3). Increasing the reaction time did not improve the reaction yield (Table 1, entry 5). During the optimization

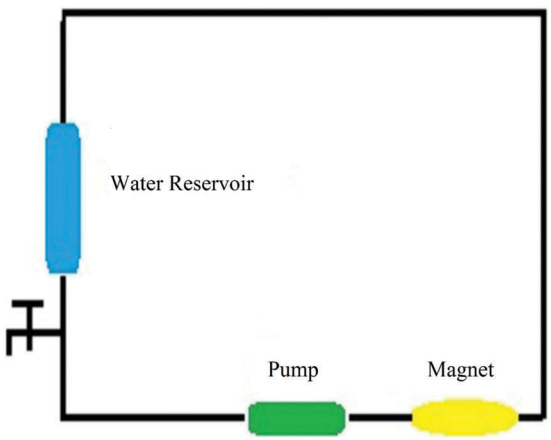

Fig. 1 Pilot for solvent magnetization apparatus.

Table 1 Synthesis of propargylamine **4a** under various conditions[a]

Entry	Solvent	Magnetization time (min)	Temp. (°C)	Reaction time (h)	Yield[b] (%)
1	MW	2	60	2	67
2	MW	5	60	2	72
3	MW	10	60	2	85
4	MW	15	60	2	80
5	MW	10	60	3	85
6	MW	10	50	2	75
7	MW	10	40	2	64
8	MW	10	25	2	50
9	MW	10	80	2	84
10	Normal water	Non-magnetized	60	5	—

[a] Reaction conditions: benzaldehyde (1 mmol), piperidine (1.2 mmol), phenyl acetylene (1.5 mmol), solvent (3 mL). [b] Isolated yield.

Table 2 Synthesis of propargylamine **4a** at different times after water magnetization[a]

Entry	Time after completion of magnetic exposure (h)	Yield[b] (%)
1	0 (freshly-magnetized water)	85
2	3	84
3	6	75
4	10	50

[a] Reaction conditions: benzaldehyde (1 mmol), piperidine (1.2 mmol), phenyl acetylene (1.5 mmol), MW (3 mL), magnetization time (10 min), reaction time (2 h), 60 °C. [b] Isolated yield.

process, the reaction temperature was varied between 25 and 80 °C with 60 °C giving the optimal reaction enhancement.

Several researchers have reported that when the applied magnetic field is removed from the MW, its magnetization effect does not disappear immediately and can be maintained for a relatively long time period. This phenomenon is referred to as the "memory effect" of MW, *i.e.* how long the water magnetization effect remains after completion of the magnetic exposure.[23] Thus we examined the memory effect of MW (Table 2).

The model reaction was performed in MW at different times after completion of the magnetic exposure. After a magnetic exposure of 10 minutes, MW was left standing for different time periods. It was found that MW kept its magnetization property for up to 3 hours, and a reaction performed in water magnetized for some time was as acceptable as that carried out in freshly-magnetized water with a high reaction yield (Table 2, entry 2).

Under the optimized reaction conditions, the scope of the reaction was explored with various alkynes, aryl aldehydes, and amines. As shown in Table 3, the reaction of phenyl acetylene with benzaldehyde and piperidine took place smoothly at 60 °C in MW to give a quantitative yield of propargylamine **4a** (entry 1). It could be concluded that aryl aldehydes bearing an electron-donating or electron-withdrawing group were obtained in good-to-high yields. Remarkably, when the reaction was carried out with terephthalaldehyde using 3 equiv. of phenyl acetylene and 2.4 equiv. of amine morpholine, piperidine or dimethylamine, only disubstituted products were obtained in 82%, 79%, and 80% yields, respectively, without the formation of any mono-substituted propargylamine (Table 3, entries 18–20). Moreover, the reaction of propargylalcohol with the more reactive electron-withdrawing *p*-chlorobenzaldehyde gave a good yield (Table 3, entries 21 and 22).

The ^{1}H NMR spectrum of **4u** shows two multiplets for the morpholine ring protons at δ 2.52 and δ 3.67, two singlets for the CH_2 and CH protons at δ 4.41 and δ 4.56, respectively, and two doublets for the aromatic ring protons at δ 7.31 and δ 7.51.

Table 3 A^3-Coupling of alkynes, aryl aldehydes, and amines in MW[a]

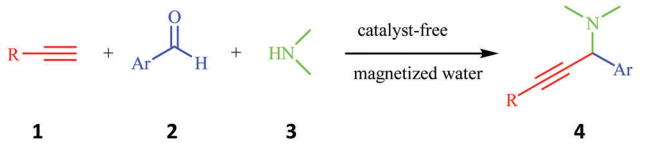

1 2 3 4

Entry	R	Ar	Amine	Product	Time (min)	Yield[b] (%)
1	Ph	Ph	Piperidine	**4a**	120	85
2	Ph	Ph	Morpholine	**4b**	125	87
3	Ph	Ph	Pyrrolidine	**4c**	140	90
4	Ph	4-$CH_3C_6H_4$	Pyrrolidine	**4d**	120	76
5	Ph	4-$CH_3C_6H_4$	Morpholine	**4e**	120	80
6	Ph	4-ClC_6H_4	Morpholine	**4f**	110	75
7	Ph	4-ClC_6H_4	Pyrrolidine	**4g**	135	78
8	Ph	2-ClC_6H_4	Morpholine	**4h**	135	65
9	Ph	2-ClC_6H_4	Piperidine	**4i**	130	68
10	Ph	2,4-$Cl_2C_6H_3$	Morpholine	**4j**	110	88
11	Ph	4-BrC_6H_4	Morpholine	**4k**	145	77
12	Ph	4-BrC_6H_4	Piperidine	**4l**	130	65
13	Ph	2-$MeOC_6H_4$	Piperidine	**4m**	135	69
14	Ph	2-OHC_6H_4	Morpholine	**4n**	160	81
15	Ph	2-OHC_6H_4	Piperidine	**4o**	155	83
16	Ph	3-$NO_2C_6H_4$	Morpholine	**4p**	150	73
17	Ph	3-$NO_2C_6H_4$	Piperidine	**4q**	130	78
18	Ph	4-$CHOC_6H_4$	Morpholine	**4r**	150	82[c]
19	Ph	4-$CHOC_6H_4$	Piperidine	**4s**	145	79[c]
20	Ph	4-$CHOC_6H_4$	Dimethylamine	**4t**	160	80[c]
21	CH_2OH	4-ClC_6H_4	Morpholine	**4u**	145	68
22	CH_2OH	4-ClC_6H_4	Diethylamine	**4v**	145	72

[a] Reaction conditions: aldehyde (1.0 mmol), amine (1.2 mmol), alkyne (1.5 mmol), magnetization time (10 min), MW (3 mL), 60 °C. [b] Isolated yield. [c] Disubstituted product.

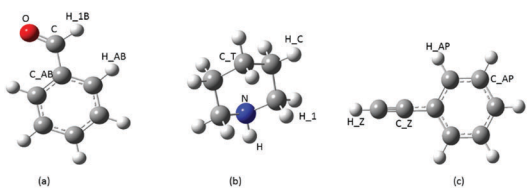

Fig. 2 Optimized structures and atomic labels for (a) benzaldehyde, (b) piperidine, and (c) phenyl acetylene (oxygen, red; carbon, dark gray; nitrogen, blue; hydrogen, light gray).

Discussion

Molecular dynamics part

Firstly, to gain a deep look at the situation, the atomic labels for each molecule are given in Fig. 2; the molecular structures and the atomic labels are given to distinguish between the different interactions that will be discussed.

In the case of molecular systems, the radial distribution function (RDF) describes the probability of finding a particle at a distance dr away from a particle in a simulation box containing N particles. As we shall see later, the present MD simulation shows that applying an external magnetic field on water, as the solvent of the reaction, changes the relative distance of the reagents, leading to a faster reaction; this positioning causes the particle to possess a much slower mobility, and therefore, a more effective interaction towards the production of propargyl amines. A more detailed exploration is given in Fig. 3. As shown in this figure, the pair correlation function of the target organic compounds was studied.

The interaction between C_AB and C, the carbon atoms of a benzaldehyde ring and a carbonyl group, gets stronger in MW since their distance gets closer after solvent magnetization from 3.875 Å to 3.825 Å. This variation in the case of the

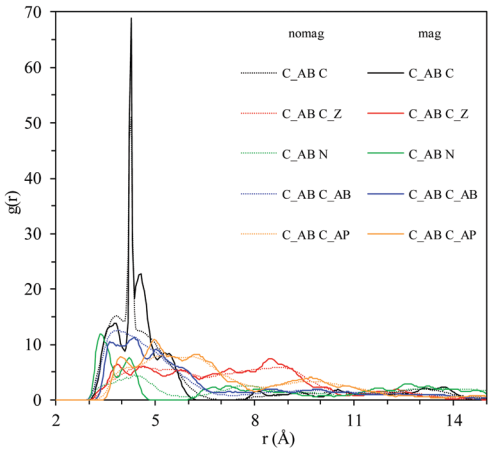

Fig. 3 Comparison between the RDFs of target organic compounds in non-magnetized water and MW (10 T).

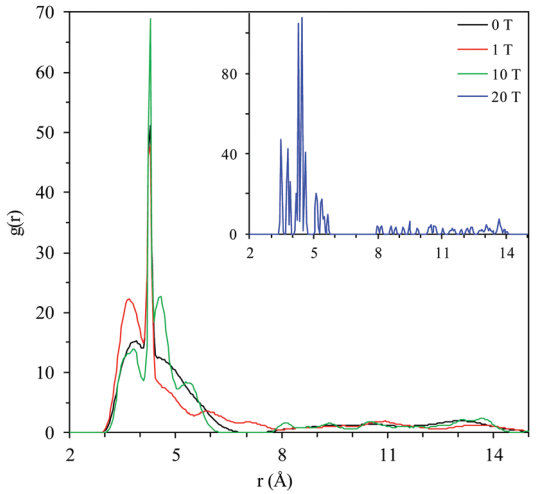

Fig. 4 Comparing RDF C_AB...C pairs for non-magnetized water and MW with strengths of 0, 1, 10, and 20 T.

C_AB and C_Z interaction corresponds to a closer distance by 0.850 Å and 0.527 in the height. Application of a magnetic field brings the C_AB from benzaldehyde and the N atom from piperidine closer together. In non-magnetized water, their distance is 4.125 Å with an intensity of 4.058, while in MW, their distance is 3.375 Å with a height of 11.841. In other words, the benzaldehyde and piperidine particles are close enough to interact strongly. Benzaldehyde molecules in both conditions, *i.e.* in non-magnetized water and MW, interact weakly since the broad peak in the former is converted to a peak with some shoulders. As a result, two benzaldehyde molecules do not enjoy a considerable interaction. Finally, the benzaldehyde and phenyl acetylene interaction *via* C_AB and C_AP is stronger due to the presence of MW; in the presence of non-magnetized water, their distance is 5.125 Å with a height of 7.927, though their distance is 3.925 Å in MW with an intensity of 7.783.

By enhancing magnetic field from weak (1 T) to strong (20 T) at the same temperature, there is not observed any considerable change. Furthermore, by increasing the magnetic flux density, the organic compounds do not interact more considerably. To highlight this point, see Fig. 4 that compares the effect of MW at different strengths (0, 1, 10, and 20 T) for the C_AB...C pair correlation.

As this figure illustrates, the enhancement in the interaction by the magnetic field does not have a linear correlation with the magnetic flux density. In addition, comparing RDFs gives the impression that in the case of the interaction between the studied organic compounds, the use of MW makes these molecules closer together from their rings. From this point of view, as illustrated in Fig. 3, due to the presence of MW, benzaldehyde, phenyl acetylene, and piperidine are closer together with stronger π–π interactions between the rings as well as strong hydrogen bonds (discussed in the next paragraph).

As one can see, the interaction between the compounds is directly affected by MW. On the other hand, each pair of atoms experiences a shell structure, *i.e.* the molecules are more ordered and stable, and their interaction is stronger than in the case of the untreated solvent. This ordered structure can be found by exploring the number of hydrogen bonds (HBs) and their strength in the system. Fig. 3 demonstrates that for the system under study, the distance between the molecules of benzaldehyde, phenyl acetylene, and piperidine decreases by approximately 1 Å, which confirms that the magnitude of the interaction effect in non-magnetized water is not equivalent to that in MW, and a marginal effect of the interaction term is observed. To evaluate the average number of HBs, the present work adopts the geometric criterion[24] that a hydrogen bond is formed if the distance between the hydrogen acceptor and the hydrogen donor atoms of a pair of molecules is less than 3.0 Å. This procedure has been applied to water molecules by Levitt *et al.*[25] The simulation results indicate that MW intensifies the HB strength. The slight decrease in the distances of the electronegative atoms O and N by MW enhances the networking ability. Moreover, near connection of the H and O atoms as well as

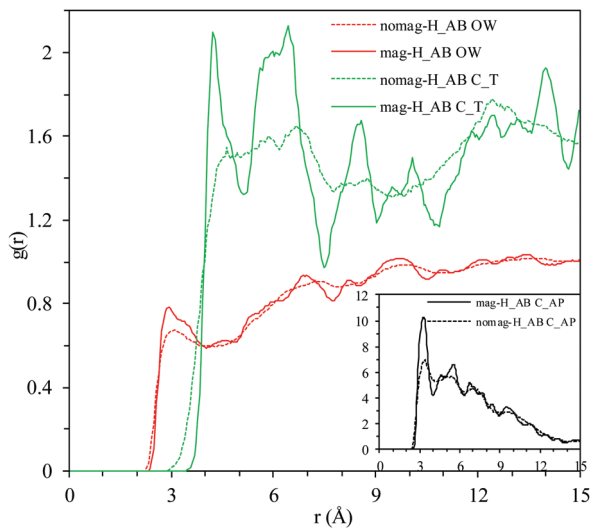

Fig. 5 Comparison between selected pair correlations with non-magnetized water and MW.

the H and N atoms of the organic compounds implies that the HB interaction is intensified by the treated solvent.

As mentioned above, not only HBs between the materials under consideration and water but also their interaction with each other enhance due to the presence of MW, which is one of the significant factors involved in the present work. Fig. 5 compares the variation in the pair correlations by applying a static magnetic field to the solvent. As illustrated in this figure, the HB power is increased by MW. However, the interaction between the studied organic compounds shows some fluctuations. To gain deeper information, the variation of HB number against the variation of configuration number was studied due to applying magnetized solvent. The number of HBs between the benzaldehyde and piperidine molecules is just one (O···H–N), and applying a magnetic field on water, as the solvent, increases the number of configurations with the ability to form a HB. In other words, the time that these two molecules are in close contact enhances. Although HBs between benzaldehyde and phenyl acetylene disappear, benzaldehyde and water enjoy a strong interaction due to magnetization, which is in accordance with the plausible mechanism. Besides, not only do the piperidine molecules witness a weaker interaction with each other but also piperidine and phenyl acetylene observe a strong interaction at a distance of 2.90 Å with a greater number of configurations than the untreated water. Finally, though piperidine experiences no HBs with benzaldehyde if a magnetic field is applied to the solvent, the number of HBs with water enhances through the simulation time. Moreover, the number of HBs between the carbonyl group and hydrogen atoms of benzaldehyde increases from 4 to 5 due to performing simulation by MW, while it changes from 14 to 16 in the case of piperidine molecules. In addition, the strong interaction between the organic reagents and water follows the reaction towards the products.

In order to compare the effect of magnetic field strength on the water–benzaldehyde interaction, as a typical sample, the RDF of atom pairs OW and H_AB was under consideration.

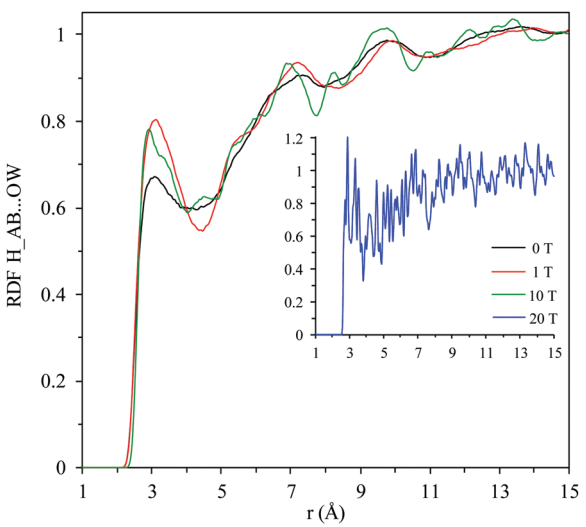

Fig. 6 RDF comparison between H_AB and OW at different magnetic field flux densities.

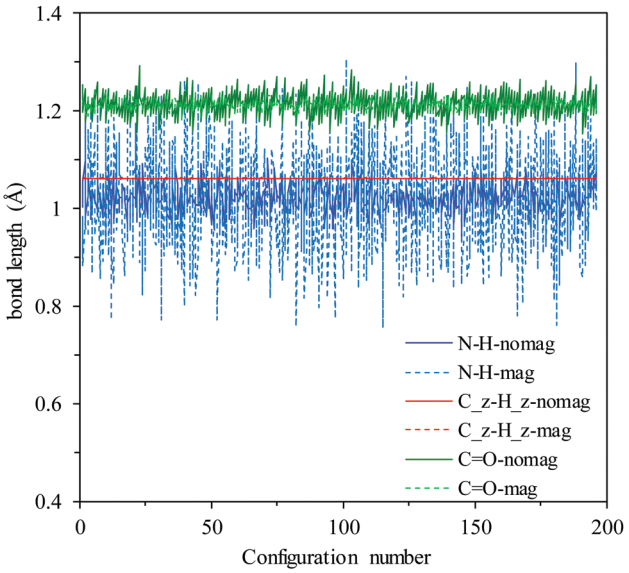

Fig. 7 Active bond changes with simulation time as a function of water magnetization (10 T).

Fig. 6 shows the RDF comparison for the mentioned atom pairs. As one can observe, the variation in HB interaction with magnetic field strength is not linear, though the high intensity magnetic field, 20 T, leads to a strong interaction; at a low flux density of the magnetic field, the trend is inversed. As a result, it should be considered how strong the magnetic field is. In summary, the simulation results illustrate that the distance between two molecules in untreated and treated water is different and a slight compactness of the bulk system due to the presence of the magnetic field is observed.

Investigation of bond strength for active bonds including the C═O, N–H, and acetylenic C–H bonds in the reaction in the absence of a magnetic field and in its presence shows that the N–H bond is more sensitive to an applied magnetic field. In other words, this bond experiences more variation during the reaction if magnetized water is applied. Fig. 7 shows the variation in active bond lengths during the simulation time in the presence of magnetized water and in its absence. As shown in the figure, the effect of magnetization on the acetylenic C–H bond is inconsiderable and its influence on the N–H bond is the most.

Simulation details

By employing the hybrid density functional theory incorporating Becke's three-parameter exchange with the Lee, Yang, and Parr's (B3LYP) correlation functional,[26] density functional theory (DFT) was performed on the pure benzaldehyde, phenyl acetylene, and piperidine systems using the Gaussian 03 program.[27] The geometry of the lowest-energy conformer was optimized at the B3LYP/6-311++G(d,p) level of theory. Here, the default criteria for convergence of the *ab initio* calculations and the geometry optimizations in the Gaussian 03 program were applied. The molecular electrostatic potential (MESP)[28] of water, as a pure solvent, was calculated to shed light on the effective localization

of electron-rich regions in the molecular system. The vibrational analysis demonstrated that all the optimized structures were at a local minimum. Consequently, the geometrical parameters including bond lengths, bond angles, and dihedral angles, computed at the B3LYP/6-311++G(d,p) level of theory as well as the atomic charges were implemented in order to construct the initial configuration for the next step, the MD simulation. The electrostatic potential surface (EPS) method[29] was applied to compute the partial atomic charges. Earlier simulation results have confirmed that the CHelpG atomic charges lead to more accurate results, which are in an excellent agreement with the experimental results obtained under ambient conditions (298.15 K and 1 bar). The OPLS (Optimized Potential for Liquid Simulations) all-atom force field,[30] which is one of the most accurate potentials for organic molecules, was applied, and the Lennard-Jones parameters were taken from previous reports.[30] It was assumed that the acetylene chain could be modeled as a rigid body, the benzene ring could be modeled as a flexible body, and all the C–H bonds in the ring rotate according to a torsional potential. Columbic interactions were modeled using fixed ESP results of DFT to compute the partial charges on the center of each atom. Long-range electrostatic interactions were accounted for using the Ewald procedure[31] within the isothermal–isobaric (*NPT*) ensemble at 298.15 K. All particles were confined in a 3D simulation box of a finite size, and the periodic boundary conditions were applied to produce image boxes that mimic the behavior of an infinitely large system. 1000 water molecules besides all the mentioned solutes (benzaldehyde, phenyl acetylene, and piperidine) with equal numbers were placed in the simulation box, and the simulation was run for a period of 1 ns in the *NPT* ensemble to adjust the simulation system, achieving a suitable density at a pressure of 1.01325 bar with a cut-off distance of 15 Å. The coupling methods for pressure and temperature were applied by a Nose-hoover thermostat–barostat every 0.1 and 1.0 ps, respectively.[32] The Leapfrog Verlet integration scheme[31e] with a time step of 1 fs was applied to compute the positions and velocities of the particles. After reaching the equilibrium state, the system was kept running for 300 ps to achieve the input for the next simulation step. In order to collect the required data with the applied potential model, the last configuration was applied for another simulation with the *NVT* (constant number of particles, constant volume, and constant temperature) ensemble. All the conditions were kept the same as those in the previous simulation. An external constant magnetic field perpendicular to the *z*-direction was applied to the pure solvent using the MD computation. All the MD simulations were conducted using the DL_POLY software, version 2.17.[33]

In the current study, we pursued the potential ''storing'' of energy from exposures to a 10.0 T static magnetic field with a constant volume of water as the solvent. It was assumed that the changes in water diffusion reflected altered viscosity explained by the molecular aspect. A sudden and protracted increase in the diffusion velocity would reflect the dissipation of stored energy or information. Correspondingly, dissipation of total stored energy was involved with altered structural, thermodynamic, and transport properties. An accurate practical means for the analysis of the structure was provided by the radial distribution function (RDF) of a pair of atoms, which is defined by the local number density, $\rho(r)$, at radius r divided by the bulk number density, ρ_0:

$$g(r) = \frac{\rho(r)}{\rho_0} = \frac{V \cdot \mathrm{d}N(r, \mathrm{d}r)}{N \cdot 4\pi r^2 \mathrm{d}r} \quad (1)$$

in which N is the number of molecules, V is the system volume, and $\mathrm{d}N(r, \mathrm{d}r)$ is the number of molecules within a shell that is between r and $r + \mathrm{d}r$ from the center of the molecule with $\mathrm{d}r = 0.1$ Å.

In an MD simulation, the diffusion coefficient for the translational motion, D, can be obtained from the mean square displacement (MSD) of molecules using the Einstein's relation, which is an indication of the diffusion phenomenon. It is defined as:

$$\mathrm{MSD} = \langle |r_j(t) - r_j(0)| \rangle^2 \quad (2)$$

where $r_j(t)$ and $r_j(0)$ denote the position vectors of atom j at time t and time 0, respectively. The rate of growth of MSD rests on the number of times that an atom suffers collisions per unit time.

Conclusions

A catalyst-free, green, efficient, and convenient method was proposed for the one-pot three-component reaction of terminal alkynes, secondary amines, and aldehydes in MW. The promising points for the presented methodology are its generality, efficiency, clean reaction profile, short reaction time, simple work-up procedure, and finally, agreement with the green chemistry protocols, making it a useful and attractive process for the synthesis of propargylamines. Furthermore, the mobility of the system reduced when treated solvent was applied, *i.e.* the magnetic field constrained the movement of the water molecules, which is in good agreement with decreasing the movement of organic reagents alongside encouraging them to keep less distance together and produce suitable products. Atom-atom pair correlation functions, made available from the histogram of trajectories, were applied to estimate the spreading profile and thus the structural relation between particles. Importantly, using MW, the system observed more variations in comparison with the stable condition of the untreated solvent. However, HB interaction was detectable as a considerable factor on the forwarding of the reaction.

Experimental

General information

The reagents used were all supplied from Merck or Fluka, and used without any further purification. Melting points were recorded on a Thermocouple digital melting point apparatus. FT-IR spectra were obtained as potassium bromide pellets in the range of 400–4000 cm^{-1} on a Bomem MB series

spectrometer. NMR spectra were recorded on a Bruker 300 MHz ^{1}H NMR, 75 MHz ^{13}C NMR spectrometer.

Preparation of magnetized water

Doubly distilled water, deionized by a Millipore Q-Plus 185 system, was used in the experiments. Therefore, there were no metallic or magnetic elements present in the purified water used. As shown in Fig. 1, a centrifugal pump was used to circulate water in the system. Water was treated in the system for 10 min, and 100 mL of MW was used in the current work.

General procedure for synthesis of propargylamines 4a–v

To a 10 mL round-bottomed flask equipped with a magnetic stirrer bar and containing MW (3 mL, with a magnetization time of 10 min), were added an aldehyde (1.0 mmol), an amine (1.2 mmol), and an alkyne (1.5 mmol). The reaction mixture was stirred at 60 °C, and the reaction progress was monitored by TLC using chloroform, as the eluent. The resulting crude product was purified by column chromatography on silica gel (eluent: hexane/ethyl acetate = 10/2) to give the corresponding product (Table 3).

4-(3-Phenyl-1-(*p*-tolyl)prop-2-yn-1-yl)morpholine 4e. Yellow solid; m.p., 78–80 °C; FT-IR (KBr): 3050 (C≡C), 2860, 2823, 1489, 1450, 1318, 1113 cm^{-1}; ^{1}H NMR ($CDCl_3$, 300 MHz): δ 2.40 (s, 3H), 2.65–2.71 (m, 4H), 3.76–3.72 (m, 4H), 4.79 (s, 1H), 7.20 (d, 2H, J = 8.0 Hz), 7.36 (d, 2H, J = 8.0 Hz), 7.52–7.60 (m, 5H); ^{13}C NMR ($CDCl_3$, 75 MHz) δ 21.2, 50.0, 61.8, 67.2, 85.5, 88.4, 123.2, 128.3, 128.4, 128.6, 129.0, 131.9, 135.0, 137.4.

4-(1-(4-Chlorophenyl)-3-phenylprop-2-yn-1-yl)morpholine 4f. Yellow oil; FT-IR (thin film): 3060 (C≡C), 2956, 1495, 1028 cm^{-1}; ^{1}H NMR ($CDCl_3$, 300 MHz): δ 2.56–2.64 (m, 4H), 3.67–3.75 (m, 4H), 4.75 (s, 1H), 7.36–7.45 (m, 5H), 7.50–7.53 (m, 2H), 7.55–7.58 (m, 2H); ^{13}C NMR ($CDCl_3$, 75 MHz): δ 49.8, 61.4, 67.1, 84.4, 88.9, 122.7, 125.5, 128.1, 128.4, 128.4, 129.7, 129.9, 131.5, 131.8, 132.1, 133.6, 135.8, 136.5.

4-(1-(2-Chlorophenyl)-3-phenylprop-2-yn-1-yl)morpholine 4h. Yellow oil; FT-IR (thin film): 3045 (C≡C), 2997, 2897, 2750, 1562, 1472, 1324, 1274, 1232, 1145, 1117, 1055 cm^{-1}; ^{1}H NMR ($CDCl_3$, 300 MHz): δ 2.62–2.67 (m, 4H), 3.70–3.77 (m, 4H), 5.10 (s, 1H), 7.25–7.29 (m, 2H), 7.33–7.36 (m, 3H), 7.40–7.42 (m, 1H), 7.50–7.54 (m, 2H), 7.73–7.75 (m, 1H); ^{13}C NMR ($CDCl_3$, 75 MHz): δ 49.8, 58.9, 67.1, 84.7, 88.4, 122.8, 125.5, 126.3, 128.3, 128.4, 129.1, 129.9, 130.5, 130.9, 131.8, 134.6, 135.5, 135.8.

4-(1-(3-Nitrophenyl)-3-phenylprop-2-yn-1-yl)morpholine 4p. Yellow oil; FT-IR (thin film): 3080 (C≡C), 3020, 2957, 2859, 1530, 1454, 1300, 1113, 1075 cm^{-1}; ^{1}H NMR ($CDCl_3$, 300 MHz): δ 2.64–2.70 (m, 4H), 3.70–3.77 (m, 4H), 4.90 (s, 1H), 7.38–7.42 (m, 3H), 7.54–7.58 (m, 3H), 8.02 (d, 1H, J = 8.0 Hz), 8.18 (d, 1H, J = 8.0 Hz), 8.50 (s, 1H); ^{13}C NMR ($CDCl_3$, 75 MHz): δ 49.7, 61.3, 66.9, 83.1, 89.7, 122.2, 122.8, 123.4, 125.5, 128.4, 128.7, 129.1, 131.9, 134.5, 140.4, 148.3.

1,4-Bis(*N*,*N*-dimethyl-3-phenylprop-2-yn-1-amine) 4t. Yellow oil; FT-IR (thin film): 3040 (C≡C), 2900, 1480 cm^{-1}; ^{1}H NMR ($CDCl_3$, 300 MHz): δ 2.30 (s, 6H), 4.90 (s, 1H), 7.29–7.37 (m, 3H), 7.53–7.56 (m, 2H), 7.65 (s, 2H); ^{13}C NMR ($CDCl_3$, 75 MHz): δ 138.0, 131.8, 129.4, 128.8, 128.4, 128.3, 88.4, 84.6, 61.9, 41.6.

4-(4-Chlorophenyl)-4-morpholinobut-2-yn-1-ol 4u. Yellow oil; FT-IR (thin film): 3400, 3055 (C≡C), 2900, 1490, 1100 cm^{-1}; ^{1}H NMR ($CDCl_3$, 300 MHz): δ 2.52–2.58 (m, 4H), 3.67–3.76 (m, 4H), 4.41 (s, 2H), 4.56 (s, 1H), 7.31 (d, 2H, J = 8.0 Hz), 7.51 (d, 2H, J = 8.0 Hz); ^{13}C NMR ($CDCl_3$, 75 MHz): δ 49.6, 50.8, 60.9, 66.9, 80.3, 87.2, 128.4, 129.8, 133.7, 135.8.

4-(4-Chlorophenyl)-4-(diethylamino)but-2-yn-1-ol 4v. Yellow oil; FT-IR (thin film): 3400, 3080 (C≡C), 2910, 1480, 1100 cm^{-1}; ^{1}H NMR ($CDCl_3$, 300 MHz): δ 1.06 (t, 6H, J = 7.2 Hz), 2.43–2.59 (m, 4H), 4.34 (d, 2H, J = 2.0 Hz), 4.85 (s, 1H), 7.33 (d, 2H, J = 8.0 Hz), 7.57 (d, 2H, J = 8.0 Hz); ^{13}C NMR ($CDCl_3$, 75 MHz): δ 14.1, 44.4, 60.2, 68.1, 81.3, 96.3, 128.8, 129.7, 132.3, 133.2.

Conflicts of interest

There are no conflicts to declare.

Acknowledgements

We wish to express our thanks to the Research Council of the Shahrood University of Technology for the financial support of this work.

References

1 D. F. Harvey and D. M. Sigano, *J. Org. Chem.*, 1996, **61**, 2268–2272.
2 Y. Yamamoto, H. Hayashi, T. Saigoku and H. Nishiyama, *J. Am. Chem. Soc.*, 2005, **127**, 10804–10805.
3 B. Yan and Y. Liu, *Org. Lett.*, 2007, **9**, 4323–4326.
4 E. S. Lee, H. S. Yeom, J. H. Hwang and S. Shin, *Eur. J. Org. Chem.*, 2007, 3503–3507.
5 (*a*) I. E. Kopka, Z. A. Fataftah and M. W. Rathke, *J. Org. Chem.*, 1980, **45**, 4616–4622; (*b*) Y. Imada, M. Yuasa, I. Nakamura and S.-I. Murahashi, *J. Org. Chem.*, 1994, **59**, 2282–2284; (*c*) T. Murai, Y. Mutoh, Y. Ohta and M. Murakami, *J. Am. Chem. Soc.*, 2004, **126**, 5968–5969; (*d*) Y. Wang, L. Jiang, L. Li, J. Dai, D. Xiong and Z. Shao, *Angew. Chem., Int. Ed.*, 2016, **55**, 15142–15146; (*e*) Y. Wang, M. Mo, K. Zhu, C. Zheng, H. Zhang, W. Wang and Z. Shao, *Nat. Commun.*, 2015, **6**, 8544.
6 C. I. Li and C. Wei, *Chem. Commun.*, 2002, 268–269.
7 R. Maggi, A. Bello, C. Oro, G. Sartori and L. Soldi, *Tetrahedron*, 2008, **64**, 1435–1439.
8 Y. Zhang, P. Li, M. Wang and L. Wang, *J. Org. Chem.*, 2009, **74**, 4364–4367.
9 S. Sakaguchi, T. Mizuta, M. Furuwan, T. Kubo and Y. Ishii, *Chem. Commun.*, 2004, 1638–1639.
10 V. K.-Y. Lo, K. K.-Y. Kung, M.-K. Wong and C.-M. Che, *J. Organomet. Chem.*, 2009, **694**, 583–591.
11 M. Bakherad, A. Keivanloo, A. H. Amin, R. Doosti and O. Hoseini, *Iran. J. Catal.*, 2016, **6**, 325–332.
12 K. Park, Y. Heo and S. Lee, *Org. Lett.*, 2013, **15**, 3322–3325.
13 S. S. Patil, S. V. Patil and V. D. Bobade, *Synlett*, 2011, 1157–1159.

14 V. S. Rawat, T. Bathini, S. Govardan and B. Sreedhar, *Org. Biomol. Chem.*, 2014, **12**, 6725–6729.
15 J. Safari, S. H. Banitaba and S. D. Khalili, *Ultrason. Sonochem.*, 2012, **19**, 1061–1069.
16 (*a*) T. Rispens and J. B. F. N. Engberts, *J. Org. Chem.*, 2002, **67**, 7369–7377; (*b*) W. Blokzijl and J. B. Engberts, *Angew. Chem., Int. Ed. Engl.*, 1993, **32**, 1545–1579.
17 (*a*) X.-F. Pang, B. Deng and B. Tang, *Mod. Phys. Lett. B*, 2012, **26**, 1250069; (*b*) F. Moosavi and M. Gholizadeh, *J. Magn. Magn. Mater.*, 2014, **354**, 239–247; (*c*) N. Gang, L. St-Pierre and M. Persinger, *Water*, 2012, **3**, 122–131; (*d*) E. Esmaeilnezhad, H. J. Choi, M. Schaffie, M. Gholizadeh and M. Ranjbar, *J. Cleaner Prod.*, 2017, **161**, 908–921.
18 K.-T. Chang and C.-I. Weng, *J. Appl. Phys.*, 2006, **100**, 043917.
19 E. Chibowski, L. Hołysz, A. Szcześ and M. Chibowski, *Colloids Surf., A*, 2003, **225**, 63–67.
20 J. Li, S. Luo, W. Yao, Z. Tang, Z. Zhang and M. Alim, *J. Eur. Ceram. Soc.*, 2004, **24**, 2605–2611.
21 T. R. Bastami and M. H. Entezari, *Ultrason. Sonochem.*, 2012, **19**, 830–840.
22 (*a*) M. Bakherad, A. Keivanloo, M. Gholizadeh, R. Doosti and M. Javanmardi, *Res. Chem. Intermed.*, 2017, **43**, 1013–1029; (*b*) M. Bakherad, R. Doosti, A. Keivanloo, M. Gholizadeh and A. H. Amin, *Lett. Org. Chem.*, 2017, **14**, 510–516; (*c*) M. Bakherad, Z. Moosavi-Tekyeh, A. Keivanloo, M. Gholizadeh and Z. Toozandejani, *Res. Chem. Intermed.*, 2017, **43**, 1–15.
23 (*a*) A. Cefalas, E. Sarantopoulou, Z. Kollia, C. Riziotis, G. Dražic, S. Kobe, J. Stražišar and A. Meden, *J. Comput. Theor. Nanosci.*, 2010, **7**, 1800–1805; (*b*) B. Deng and X. Pang, *Chin. Sci. Bull.*, 2007, **52**, 3179–3182.
24 I. Benjamin, *J. Chem. Phys.*, 1992, **97**, 1432–1445.
25 M. Levitt, M. Hirshberg, R. Sharon, K. E. Laidig and V. Daggett, *J. Phys. Chem. B*, 1997, **101**, 5051–5061.
26 (*a*) A. D. Becke, *Chem. Phys.*, 1992, **96**, 2155–2160; (*b*) C. Lee, W. Yang and R. G. Parr, *Phys. Rev. B: Condens. Matter Mater. Phys.*, 1988, **37**, 785–789.
27 M. Frisch, G. W. Trucks, H. B. Schlegel, G. E. Scuseria, M. A. Robb, J. R. Cheeseman, J. A. Montgomery, T. Vreven, K. N. Kudin, J. C. Burant, J. M. Millam, S. S. Iyengar, J. Tomasi, V. Barone, B. Mennucci, M. Cossi, G. Scalmani, N. Rega, G. A. Petersson, H. Nakatsuji, M. Hada, M. Ehara, K. Toyota, R. Fukuda, J. Hasegawa, M. Ishida, T. Nakajima, Y. Honda, O. Kitao, H. Nakai, M. Klene, X. Li, J. E. Knox, H. P. Hratchian, J. B. Cross, V. Bakken, C. Adamo, J. Jaramillo, R. Gomperts, R. E. Stratmann, O. Yazyev, A. J. Austin, R. Cammi, C. Pomelli, J. W. Ochterski, P. Y. Ayala, K. Morokuma, G. A. Voth, P. Salvador, J. J. Dannenberg, V. G. Zakrzewski, S. Dapprich, A. D. Daniels, M. C. Strain, O. Farkas, D. K. Malick, A. D. Rabuck, K. Raghavachari, J. B. Foresman, J. V. Ortiz, Q. Cui, A. G. Baboul, S. Clifford, J. Cioslowski, B. B. Stefanov, G. Liu, A. Liashenko, P. Piskorz, I. Komaromi, R. L. Martin, D. J. Fox, T. Keith, A. Laham, C. Y. Peng, A. Nanayakkara, M. Challacombe, P. M. W. Gill, B. Johnson, W. Chen, M. W. Wong, C. Gonzalez and J. A. Pople, *Gaussian 03, Revision C.0*, 2016.
28 J. S. Murray and K. Sen, *Molecular electrostatic potentials: concepts and applications*, Elsevier, 1996.
29 C. M. Breneman and K. B. Wiberg, *J. Comput. Chem.*, 1990, **11**, 361–373.
30 (*a*) W. L. Jorgensen, D. S. Maxwell and J. Tirado-Rives, *J. Am. Chem. Soc.*, 1996, **118**, 11225–11236; (*b*) S. Gautam, S. Mitra, R. Mukhopadhyay and S. Chaplot, *Phys. Rev. E: Stat., Nonlinear, Soft Matter Phys.*, 2006, **74**, 041202.
31 (*a*) M. Kohagen, M. Brehm, J. Thar, W. Zhao, F. Müller-Plathe and B. Kirchner, *J. Phys. Chem.*, 2010, **115**, 693–702; (*b*) O. Guvench, S. N. Greene, G. Kamath, J. W. Brady, R. M. Venable, R. W. Pastor and A. D. Mackerell, *J. Comput. Chem.*, 2008, **29**, 2543–2564; (*c*) L. Weng, C. Chen, J. Zuo and W. Li, *J. Phys. Chem. A*, 2011, **115**, 4729–4737; (*d*) C. Chen, W. Z. Li, Y. C. Song and J. Yang, *J. Mol. Liq.*, 2009, **146**, 23–28; (*e*) M. Allen and D. Tildesley, *Computer simulation liquids*, New York, Oxford, 1989.
32 S. Melchionna, G. Ciccotti and B. Lee Holian, *Mol. Phys.*, 1993, **78**, 533–544.
33 W. Smith and T. Forester, *J. Mol. Graphics*, 1996, **14**, 136–141.

